https://doi.org/10.53964/jmn.2025001

https://www.innovationforever.com

Journal of Modern Nanotechnology

ISSN 2788-8118 (Online)

Open Access

Research Article

Mn-Doped CdS Thin Film Deposition on FTO and Si: A Comparative Investigation

Madhavi Sharad Darekar[1*], Praveen Beekanahalli Mokshanatha[1]

[1]Department of Chemistry, Institute of Engineering and Technology, Srinivas University, Mukka, India

[*]**Correspondence to: Madhavi Sharad Darekar, Ph.D. in Physics, Post Doctorate in Nanotechnology, Post Doctorate in Physics,** Department of Chemistry, Institute of Engineering and Technology, Srinivas University, Mukka, Surathkal, Mangalore - 574146, Karnataka, India; Email: darekar.madhavi@rediff.com

Received: April 20, 2025 **Revised:** May 9, 2025 **Accepted:** May 26, 2025 **Published:** June 26, 2025

Abstract

Objective: In the present paper, the attempts were made to demonstrate the similarity between the experimental results of thin films prepared by the deposition of manganese (Mn) doped cadmium sulphide (CdS) nanoparticles on FTO glass substrates and on silicon wafers. Both these thin films have been used in the fabrication of the optoelectronic and photovoltaic devices and also in the DMS applications.

Method: The non-aqueous chemical method was used to synthesize the Mn doped CdS (CdS:Mn) diluted magnetic semiconductor (DMS) nanoparticles at room temperature. Thioglycerol was used as the capping agent to avoid the coalescence of the particles. The Mn doped CdS thin films were prepared by the deposition of Mn doped CdS nanoparticles on silicon wafers and also on fluorine doped tin oxide (FTO) glass substrates using the dip coating method. These CdS:Mn thin films were investigated by using the various analysis techniques like scanning electron microscopy (SEM), energy dispersive analysis by X-rays (EDAX), mapping, transmission electron microscopy (TEM), atomic force microscopy (AFM), ultraviolet-visible (UV-Vis) absorption spectroscopy, photoluminescence (PL) and X-ray diffraction (XRD). The cubic structure, the polycrystalline nature and the sizes of CdS:Mn nanoparticles have been observed by AFM, SEM, TEM and XRD characterization techniques. The elemental composition in CdS:Mn thin films was analyzed by EDAX technique.

Results: The particle size was decreased with increasing the Mn concentration. The characterization techniques like UV-Vis absorption and PL spectroscopy were used to study the optical properties of CdS:Mn nanoparticles. UV-Vis absorption measurements of the CdS:Mn thin films showed a blue shift in the spectra, while the PL spectra exhibited a red shift. Based on the XRD data, the CdS:Mn nanoparticles were found to have a cubic crystal structure. AFM imaging revealed a high density of rectangular clusters in CdS:Mn thin films, with these cluster sizes demonstrably increasing with longer dip times. Selected Area Electron Diffraction (SAED) patterns, exhibiting ring structures, confirmed the polycrystalline nature of the CdS:Mn thin films. Furthermore, as magnification was increased TEM analysis revealed an increase in the size of the spherical clusters visualized within these films. It was visually confirmed by SEM analysis of Mn doped CdS thin films that, heat treatment in an air atmosphere, particularly with longer dip times, increased the grain size significantly and reduced the crystal defects. The thin films exhibited near-stoichiometric compositions as determined by EDAX analysis.

Conclusion: The characterization results of CdS:Mn thin films deposited on both FTO glass and silicon substrates were similar, demonstrating the potential of Mn-doped CdS thin films for photovoltaic and optoelectronic devices due to their semiconducting properties.

Keywords: synthesis, characterization, non-aqueous chemical method, CdS:Mn nanoparticles, CdS:Mn thin films, dip coating method

Citation: Darekar MS, Praveen BM. Mn-Doped CdS Thin Film Deposition on FTO and Si: A Comparative Investigation. *J Mod Nanotechnol*, 2024; 5: 1. DOI: 10.53964/jmn.2025001.

1 INTRODUCTION

The magnetic elements such as Co, Ni, Mn, Cr, Fe etc. used as the dopants for the most important II-VI group diluted magnetic semiconductor (DMS) nanoparticles like CdS, CdSe, ZnS, etc. which can be used in various technological, magneto-optical and biomedical applications due to the changes in their electrical, magnetic, physical, optical, chemical, structural properties[1,2]. The interaction between the spin induced magnetic moment of the transition metal ions substituting the host cations and the conduction and the valence band electrons are the unique properties of the nanoparticles which are different from the bulk materials[3]. The DMS nanoparticles have large potential applications in fields like magnetic, optoelectronic, biological fields, spintronics[4], environmental areas, ferro fluid technology, spin valves, magneto caloric refrigeration, magnetic resonance imaging, material science, high density recording media etc[5]. Multifunctional magnetic nanoparticles have biomedical applications in magnetic hyperthermia treatment, target drug delivery, magnetic resonance imaging etc[5].

In this study, the non-aqueous chemical method was used to synthesize thioglycerol capped Mn doped CdS (CdS:Mn) nanoparticles with a change in the Wt.% of manganese element at room temperature. Very simple and comparatively cheaper dip coating method was used to deposit CdS:Mn nanoparticles on Fluorine doped Tin Oxide (FTO) glass substrates and silicon wafers for the preparation of CdS:Mn thin films. These thin films were characterized by Scanning Electron Microscopy (SEM), Energy Dispersive Analysis by X-rays (EDAX), Mapping, Transmission Electron Microscopy (TEM) and Atomic Force Microscopy (AFM) techniques. The topography, surface roughness and morphological study have been done by SEM, TEM and AFM. The TEM images showed the particle sizes and the selected area electron diffraction (SAED) patterns showed the polycrystalline nature of Mn doped CdS nanoparticles. The presence of the elements in doped nanoparticles in weight percentage and atomic percentage was shown by the EDAX analysis technique. In this work, the comparative study of the characterization results of CdS:Mn thin films deposited on FTO glass substrates and silicon wafers was carried out. This type of comparison was not reported in the previous literature. Due to the decrease in the particle size, these thin films are used in the fabrication of photonic devices, small size spin and charge-based devices etc[4]. These thin films can be used in novel magneto-optical applications due to their strong magneto-optical properties[4].

2 MATERIALS AND METHODS

The simple chemical route was used to synthesize CdS:Mn nanoparticles having various molarities of manganese chloride ($MnCl_2$) at room temperature in our previous work[6,7]. CdS:Mn semiconductor nanoparticles were synthesized using a cost-effective, non-aqueous chemical approach at room temperature, utilizing thioglycerol as a capping agent while maintaining a nitrogen atmosphere throughout the process[6-10]. Thioglycerol is used as a capping agent in the synthesis of Mn doped CdS nanoparticles to prevent agglomeration and promote a controlled growth of the nanoparticles. It acts as a stabilizer, coating the surface of the nanoparticles and preventing them from clumping together during the synthesis process. Additionally, thioglycerol can also act as a catalyst, aiding in the reaction process. Thioglycerol's presence on the surface of the nanoparticles creates steric hindrance, preventing them from coming into close contact and aggregating. This ensures that the nanoparticles remain dispersed and relatively uniform in size. By controlling the interaction between the nanoparticles and the synthesis medium, thioglycerol helps to regulate the growth and size of the CdS:Mn nanoparticles. In some synthesis methods, thioglycerol can also act as a catalyst, facilitating the reaction and leading to the faster formation of the nanoparticles. In essence, thioglycerol's role is crucial for producing well-defined, monodisperse CdS:Mn nanoparticles with desired properties, making it a valuable capping agent in their synthesis[6-16].

Cadmium acetate [$Cd(CH_3COO)_2$], manganese chloride ($MnCl_2$), thioglycerol [$SHCH_2CH(OH)CH_2OH$], and sodium sulfide (Na_2S) were the primary ingredients participated in the synthesis of the Mn doped CdS nanoparticles. Solutions of these Analytical Reagent (A.R.) grade chemicals were prepared in ethanol (C_2H_5OH), a non-aqueous solvent, for the synthesis of Cd:Mn semiconductor nanoparticles. By adjusting the concentration of manganese chloride and by keeping the molarities of cadmium acetate,

thioglycerol and sodium sulphide constant, CdS:Mn nanoparticles with a range of sizes and energy gaps were produced. The molarity of manganese chloride varies across the samples, being 0.080M in sample 1, 0.055M in sample 2, 0.070M in sample 3, and 0.060M in sample 4.

The reaction vessel was charged with a 25mL solution of 0.1M cadmium acetate in ethanol, which was then stirred magnetically. After a thirty-minute delay, the manganese chloride solution (0.080M in 25mL ethanol) was introduced into an equalizing device and added slowly, drop wise, to the cadmium acetate solution. The resulting mixture was then stirred. Following a two-hour reaction time, a 0.952M solution of thioglycerol in 25mL ethanol was slowly added to the mixture, which was then stirred for an additional two hours. To the previous solution, a non-aqueous sodium sulphide solution (0.1M in 25mL ethanol) was added gradually, followed by stirring for four hours. To ensure the integrity of the reactions, fresh solutions were employed. The use of a nitrogen atmosphere and room temperature during synthesis ensured that the nanoparticles were not oxidized. The colloidal solution was then subjected to reduced pressure evaporation using a rotary evaporator to concentrate it. The concentrated solution was treated with 2-propanol to promote flocculation. The sample was centrifuged to separate the supernatant and precipitate. After precipitation, 40 ml of 2-propanol was added, and the mixture was stirred for 3 hours at room temperature. The mixture was centrifuged to pellet the precipitate, leaving the supernatant and potentially removing contaminants by separating the components based on density. The precipitate was sequentially washed with acetone three times, followed by diethyl ether three times. The dried precipitate, obtained via vacuum evaporation, resulted in the Mn doped CdS nanoparticles (sample 1) in powder form[6,7]. Samples 2, 3, and 4, also prepared as CdS:Mn nanoparticles in powder form, utilized the same method.

The wet chemical deposition technique, the dip coating method was employed for the deposition of Mn doped CdS thin films on silicon wafers and FTO glass substrates. The dip coating method was used for the deposition of Mn doped CdS thin film (sample 1) approximately 150nm in thickness on the FTO glass substrate with 1500 dip times[7-10]. Sample 1 was prepared by the deposition of Mn doped CdS nanoparticles (sample J) synthesized in our previous work[6,7]. The 10mm×10mm×2mm FTO glass substrate was subjected to an ultrasonic cleaning process. This involved immersion in a solution of soap and double distilled water for 10-15 minutes, followed by separate 10-15 minute ultrasonic cleans in acetone and double distilled water. The FTO glass substrate was then placed in an oven and dried at 100°C. By mixing Mn-doped CdS nanoparticle powder with ethanol within a beaker, the precursor solution was formed. By partially immersing the beaker containing the ethanol-suspended Mn doped CdS nanoparticle powder into an ultrasonicator, the nanoparticles were kept in suspension, effectively preventing them from settling to the bottom. The pre-cleaned FTO glass substrate for Sample 1 was vertically immersed in the precursor solution, and the substrate was then lifted out after CdS:Mn nanoparticle deposition. Sample 1 was prepared by 1500 dips. After depositing nanoparticles onto the FTO glass substrate, it was dried under an IR lamp before being subjected to a 420°C heat treatment in air for 20 minutes. Following the same procedure, thin films of CdS:Mn nanoparticles were formed on the pre-cleaned FTO glass substrates[6,7].

Similarly, Mn doped CdS thin film (sample 2) approximately 330nm in thickness was deposited on FTO glass substrate with 3,300 dip times. The estimation of the thicknesses of Mn doped CdS thin films were done by using the laser profilometer[7-10]. Sample 2 was prepared by the deposition of Mn doped CdS nanoparticles (sample B) synthesized in our previous work[6,7]. Similar procedure was followed while depositing Mn doped CdS thin films (sample 3 and sample 4) on silicon wafers. Then the FTO substrates and silicon wafers were dried by keeping them under the infrared (IR) lamp. These substrates and silicon wafers were investigated using XRD, SEM, EDAX, TEM and AFM techniques after heat treatment in air atmosphere at 420°C for 20 minutes. The crystal defects, the resistivities and the band gaps of the CdS:Mn films had reduced and the particle size, the surface roughness and the crystallinity of the films had increased by the heat treatment in air atmosphere[6-8]. The band gap was reduced and the cluster size and the thickness of the films were increased with an increase in the dip time[7-10].

3 RESULTS AND DISCUSSION

3.1 Atomic Force Microscopy

Figure 1 shows the 2D and 3D AFM images of the dip coating deposited Mn doped CdS thin films (sample 1 and sample 2). Figure 2 shows the 2D and 3D AFM images of the dip coating deposited Mn doped CdS thin films (sample 3 and sample 4). The rectangular grains of various sizes were observed in the 2D AFM images of the thin films deposited on FTO glass substrates (sample 1 and sample 2) and silicon wafers (sample 3 and sample 4). Hills and valleys were observed in the 3D AFM images of both kinds of thin films. The sizes of the clusters observed in the 3D AFM images of sample 1 (Figure 1B) and sample 2 (Figure 1D) are 16.20nm and 90.91nm respectively. The sizes of the clusters observed in the 3D AFM images of sample 3 (Figure 2B) and sample 4 (Figure 2D) are 59.55nm and 209.9nm respectively. From this discussion, it is clearly observed that the clusters of Mn doped CdS thin films deposited on FTO glass substrates (sample 1 and sample 2) are small compared to the clusters of Mn doped CdS thin films deposited on silicon wafers (sample 3 and sample 4). The heights of the hills observed in the 3D AFM images of sample 1 and sample 2 are smaller than those observed in the 3D AFM images of sample 3 and

https://doi.org/10.53964/jmn.2025001

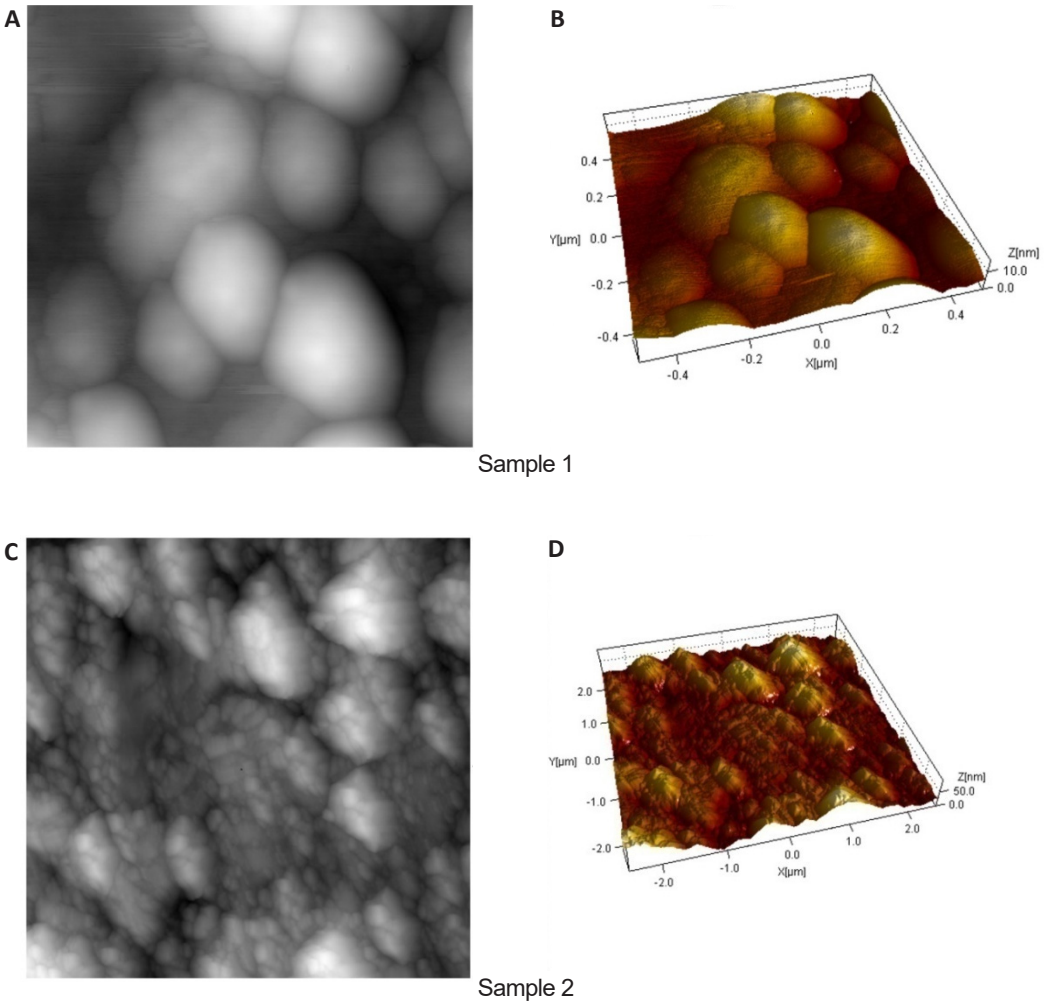

Figure 1. AFM Characterization of Mn Doped CdS Thin Films. (A) 2D Image of Sample 1, (B) 3D Image of Sample 1, (C) 2D Image of Sample 2, (D) 3D Image of Sample 2. Magnifications: 1μm for Sample 1, 5μm for Sample 2.

sample 4. This is due to the variation in the thickness of the films with the dip time[7,17].

The thickness of sample 1 is lower than that of sample 3 for the same dip time (1,500 dip times). Similarly, the thickness of sample 2 is smaller than that of sample 4 for the same dip time (3,300 dip times). From these 2D and 3D AFM observations, it is clearly seen that sample 1 and sample 2 consist of small sized clusters and short hills due to the discontinuous deposition which controls the cluster size and hill elevations and sample 3 and sample 4 consist of large sized clusters and large hill elevations due to the continuous deposition[7,17]. This means that the surface roughness of sample 1 and sample 2 is higher than that of sample 3 and sample 4 due to the growth of the initial nucleation with each dip[7,17]. The continuous deposition in case of sample 3 and sample 4 makes the film surface smooth due to the large number of nucleation and the large growth of clusters[7,17].

3.2 Transmission Electron Microscopy

The TEM images and the SAED patterns of Mn doped CdS thin films (sample 1 and sample 2) are shown in Figure 3, and the TEM images and the SAED patterns of Mn doped CdS thin films (sample 3 and sample 4) are shown in Figure 4. The uniform films without cracks are observed in the TEM images of all the samples. The SAED patterns indicate the polycrystalline nature of all the samples with the indexed planes (111) and (220) of cubic phase which are in agreement with the XRD planes of Mn doped CdS nanoparticles[6-10]. There is a difference in the orientation of atoms in different clusters[5]. The spherical clusters which are composed of polycrystalline CdS:Mn nanoparticles at several magnifications exhibit an average size increases to 66.49nm in sample 1, 99.15nm in sample 2,137.2nm in sample 3 and 213.6nm in sample 4.

3.3 Scanning Electron Microscopy

The SEM image and the SEM image (colour image) of Mn doped CdS thin film (sample 1) including the various elements are shown in Figure 5. The various elements present in sample 1 are shown in Figure 6. As shown in Figure 5, the cluster size of sample 1 decreases with an increase in the concentration of manganese element. This SEM result was confirmed by the Ultraviolet-Visible (UV-Vis) absorption analysis of Mn doped CdS nanoparticles (sample J)[6,7]. The uniform distribution of the particles is observed in the SEM image of sample 1.

https://doi.org/10.53964/jmn.2025001

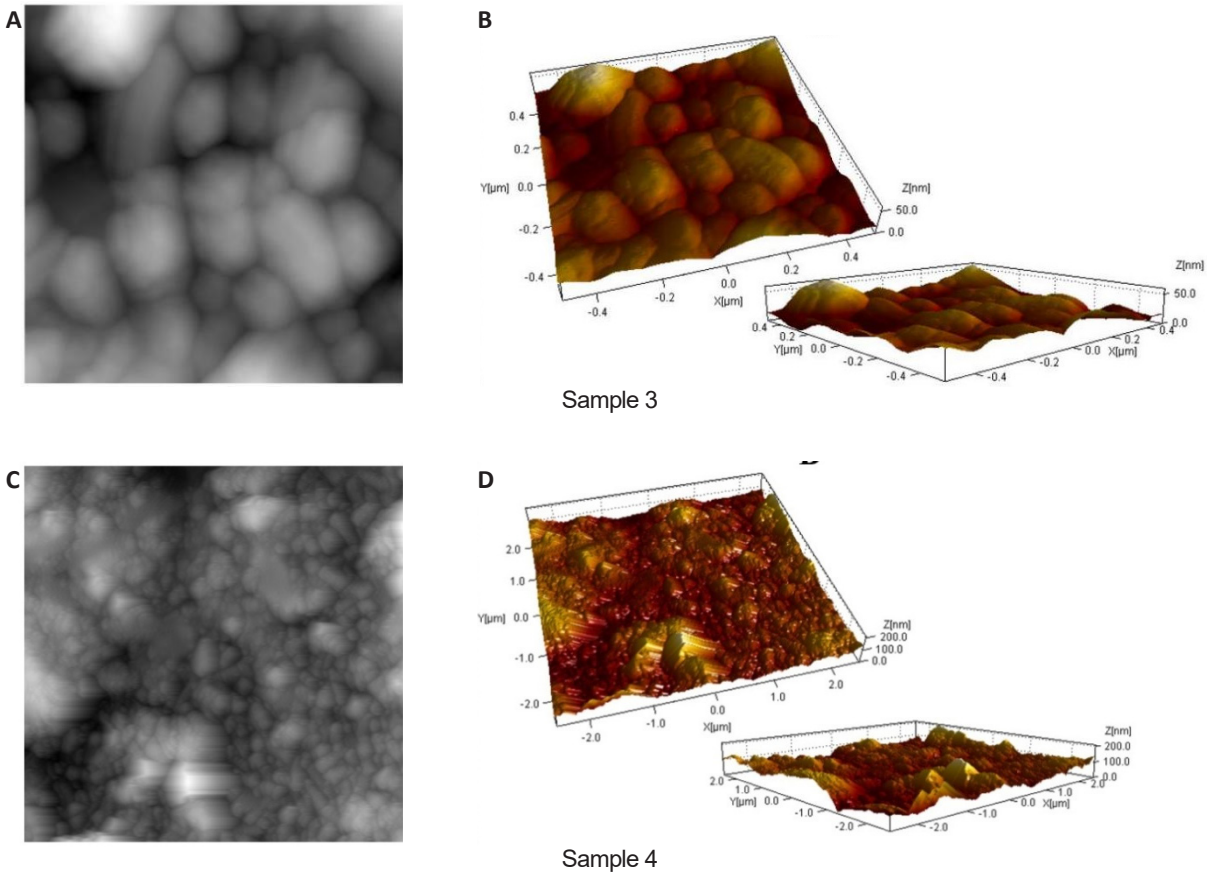

Figure 2. AFM Characterization of Mn Doped CdS Thin Films. (A) 2D Image of Sample 3, (B) 3D Image of Sample 3, (C) 2D Image of Sample 4, (D) 3D Image of Sample 4. (Magnifications: 1μm for Sample 3, 4μm for Sample 4).

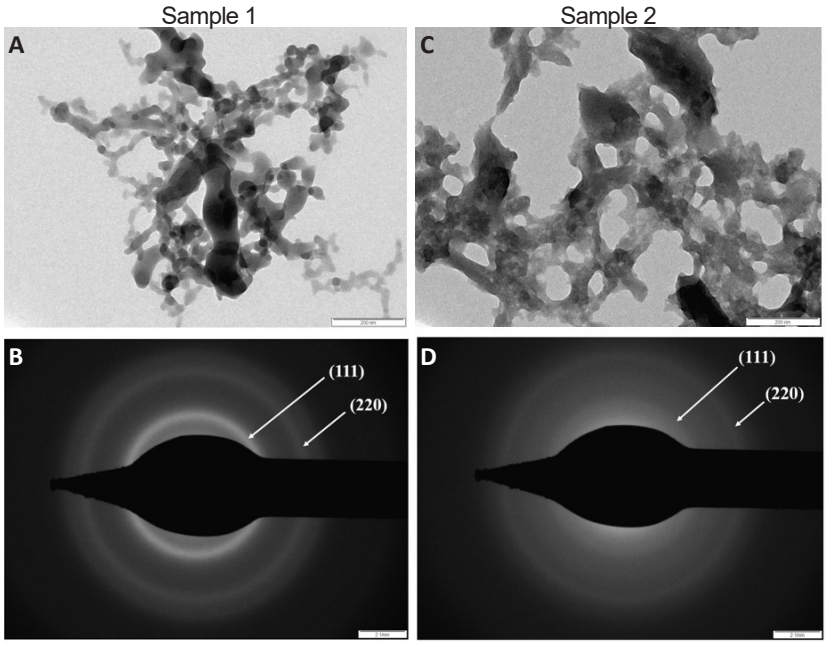

Figure 3. The TEM Images and the SAED Patterns of Mn Doped CdS Thin Films (Sample 1 And Sample 2). (A) TEM Image with Magnification of 200nm of Sample 1, (B) SAED Pattern of Sample 1, (C) TEM Image with Magnification of 200nm of Sample 2, (D) SAED Pattern of Sample 2.

The SEM image and the SEM image (colour image) of Mn doped CdS thin film (sample 2) including the various elements are shown in Figure 7. The various elements present in sample 2 are shown in Figure 8.

The SEM image and the SEM image (colour image) of Mn doped CdS thin film (sample 3) including the various elements are shown in Figure 9. The various elements present in sample 3 are shown in Figure 10.

https://doi.org/10.53964/jmn.2025001

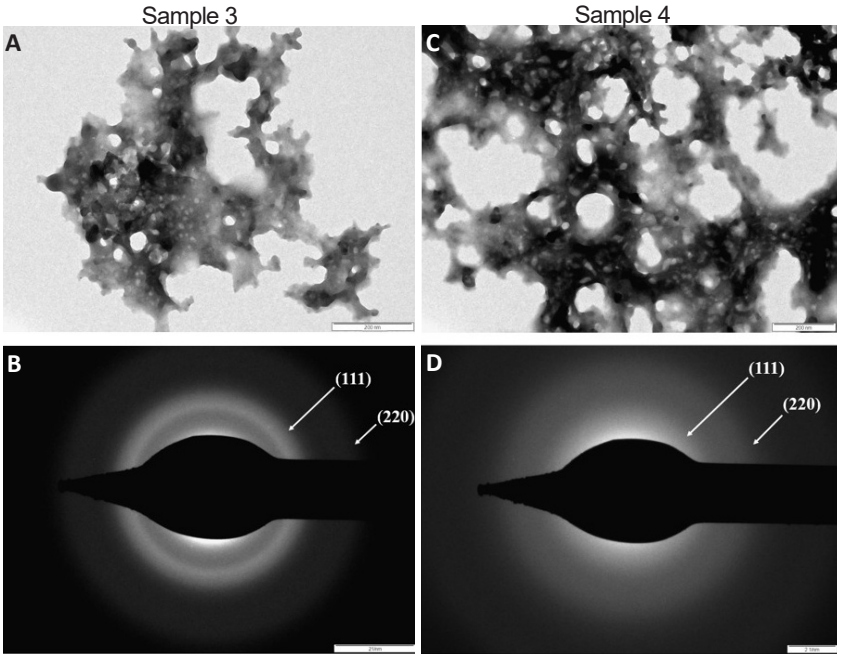

Figure 4. The TEM Images and the SAED Patterns of Mn Doped CdS Thin Films (Sample 3 And Sample 4). (A) TEM Image with Magnification of 200nm of Sample 3, (B) SAED Pattern of Sample 3, (C) TEM Image with Magnification of 200nm of Sample 4, (D) SAED Pattern of Sample 4.

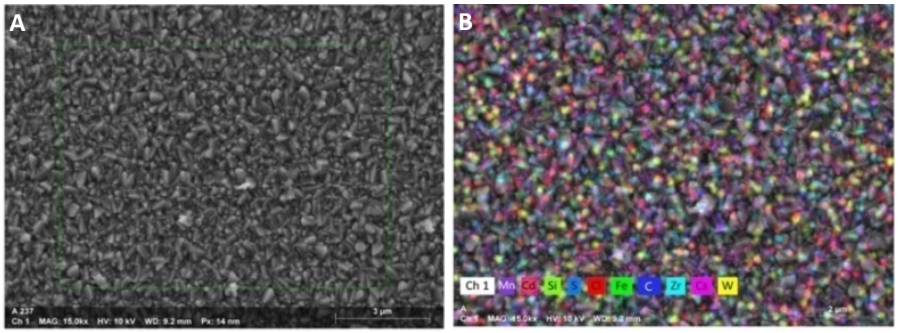

Figure 5. Mn Doped CdS Thin Film (Sample 1). (A) SEM Image with Magnification of 15,000, Scale Bar: 3μm, (B) SEM Image (Colour Image) with Magnification of 15,000. (Scale Bar: 2μm).

The SEM image and the SEM image (colour image) of Mn doped CdS thin film (sample 4) including the various elements are shown in Figure 11. The various elements present in sample 5 are shown in Figure 12.

The SEM technique was used to study the surface topography and the surface morphology of the Mn doped CdS thin films. The spongy and rough surface morphology is observed in the SEM images of Mn doped CdS thin films (sample 2, sample 3 and sample 4). The average size of the cylindrical clusters varies from 12.38 to 66.49nm in sample 1, from 26.96 to 99.15nm in sample 2, from 31.26 to 137.2nm in sample 3 and from 45.55 to 213.6nm in sample 4 with an increase in the number of dip time, the film thickness and by the heat treatment in air atmosphere. The band gap of the CdS:Mn thin films consisting of small sized cylindrical clusters of roughly 12-213nm is higher than that of the bulk CdS material due to the quantum size effect[6,7]. The non-uniform distribution of the particles is seen in the SEM micrographs of samples 2, 3 and 4. From the SEM micrographs, it is observed that the large sized clusters having cylindrical form are obtained and the crystal defects are decreased with increasing the number of dip time and the annealing temperature. The cluster sizes of CdS:Mn thin films are in nm range[7-10].

3.4 Energy Dispersive Analysis by X-rays

EDAX and mapping are the tools which were used for the analysis of elemental composition. The EDAX spectrum of dip coating deposited CdS:Mn thin film (sample 1) is shown in Figure 13. The elements like manganese (Mn), cadmium (Cd), sulphur (S), carbon (C), oxygen (O), tin (Sn) etc. present in sample 1 in stoichiometric atomic percentage are given in Table 1 and those elements are shown by Figure 6. The presence of the other elements like carbon, oxygen, tin etc. is due to the FTO glass substrate.

The EDAX spectrum of dip coating deposited CdS:Mn

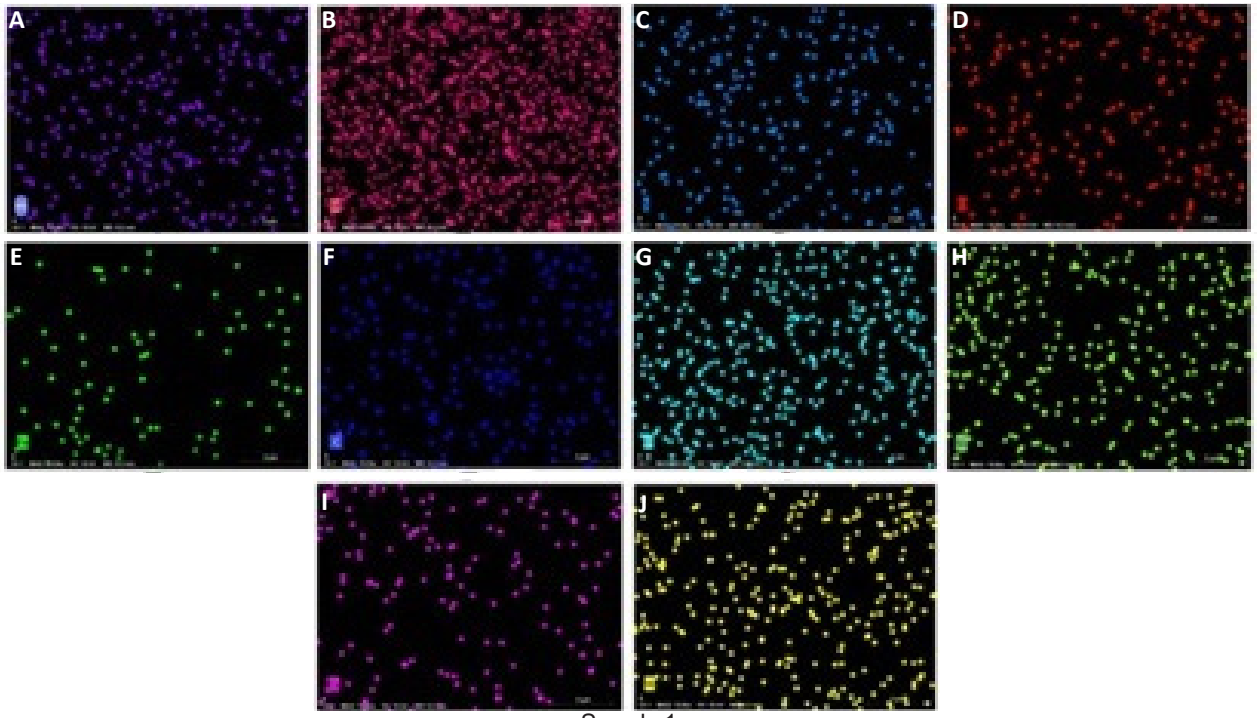

Sample 1

Figure 6. The Various Elements Present in Sample 1. (A) Manganese, (B) Cadmium, (C) Sulphur, (D) Chlorine, (E) Iron, (F) Carbon, (G) Oxygen, (H) Tin, (I) Cesium, (J) Tungsten etc. Present in Mn Doped CdS Thin Film (Sample 1) with Magnification of 15,000. (Scale Bar: 2μm).

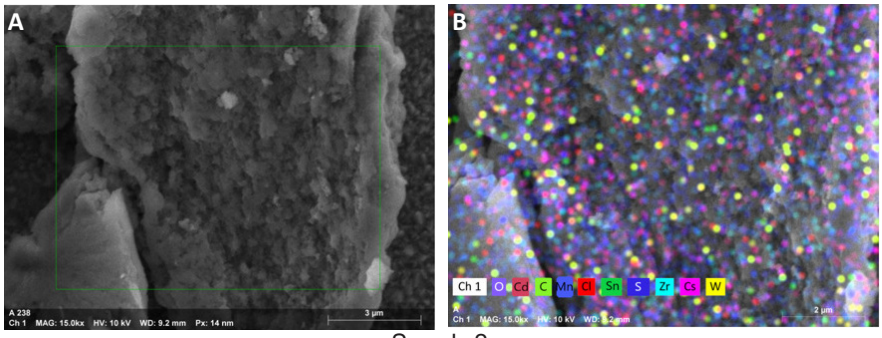

Sample 2

Figure 7. Mn Doped CdS Thin Film (Sample 2). (A) SEM Image with Magnification of 15,000, Scale Bar: 3μm, (B) SEM Image (Colour Image) with Magnification of 15,000. (Scale Bar: 2μm).

thin film (sample 2) is shown in Figure 14. The elements like oxygen (O), cadmium (Cd), manganese (Mn), sulphur (S), tin (Sn), carbon (C), chlorine (Cl) etc. present in sample 2 in stoichiometric atomic percentage are given in Table 2 and those elements are shown by Figure 8. The presence of the other elements like tin, carbon etc. is due to the FTO glass substrate.

The EDAX spectrum of dip coating deposited CdS:Mn thin film (sample 3) is shown in Figure 15. The elements like carbon (C), sulphur (S), cadmium (Cd), manganese (Mn), silicon (Si), sodium (Na), chlorine (Cl) etc. present in sample 3 in stoichiometric atomic percentage are given in Table 3 and those elements are shown by Figure 10. The presence of the other elements like carbon, silicon etc. is due to the silicon wafer.

The EDAX spectrum of dip coating deposited CdS:Mn thin film (sample 4) is shown in Figure 16. The elements like sulphur (S), cadmium (Cd), silicon (Si), carbon (C), chlorine (Cl), sodium (Na), oxygen (O), manganese (Mn) etc. present in sample 4 in stoichiometric atomic percentage are given in Table 4 and those elements are shown by Figure 12. The presence of the other elements like silicon, carbon, oxygen etc. is due to the silicon wafer.

From the EDAX spectra of CdS:Mn thin films, it is clearly seen that the intensity of the Mn peak increases with an increase in the concentration of Mn element. It is clearly observed that the samples 1, 2, 3 and 4 are rich in Cd element compared to S element. The values of Cd:S ratios for CdS:Mn thin films (sample 1 and sample 2) are 2.02 and 2.11 respectively. The values of Cd:S ratios

https://doi.org/10.53964/jmn.2025001

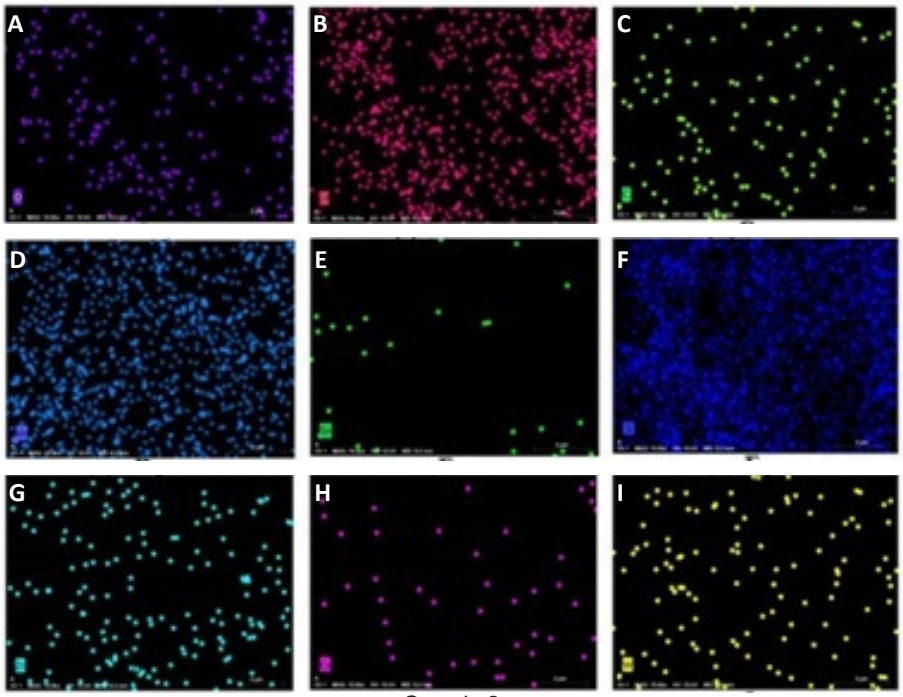

Sample 2

Figure 8. The Various Elements Present in Sample 2. (A) Oxygen, (B) Cadmium, (C) Carbon, (D) Manganese, (E) Tin, (F) Sulphur, (G) Zirconium, (H) Cesium, (I) Tungsten etc. Present in Mn Doped CdS Thin Film (Sample 2) with Magnification of 15,000. (Scale Bar: 2μm).

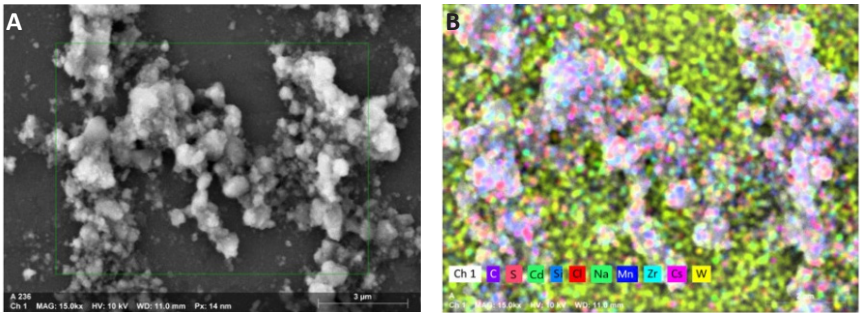

Sample 3

Figure 9 Mn Doped CdS Thin Film (Sample 3). (A) SEM Image with Magnification of 15,000, Scale Bar: 3μm, (B) SEM Image (Colour Image) with Magnification of 15,000. (Scale Bar: 2μm).

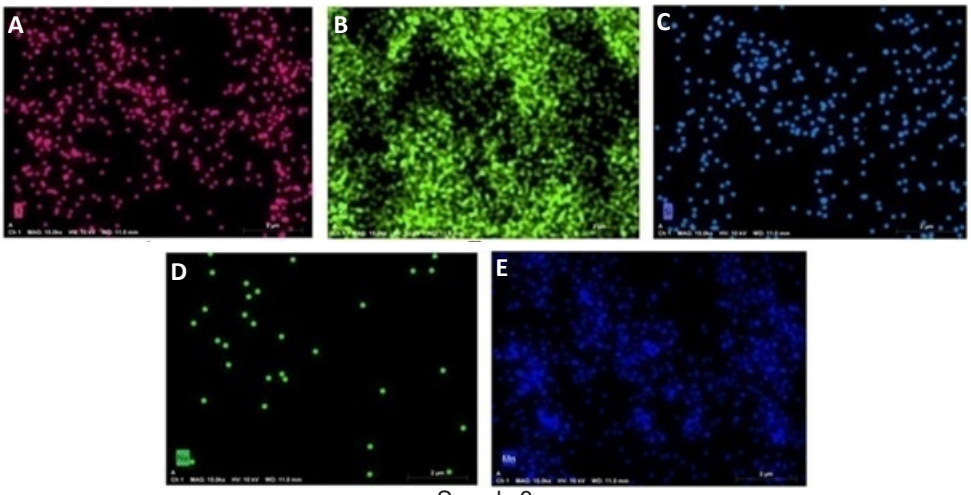

Sample 3

Figure 10. The Various Elements Present in Sample 3. (A) Sulphur, (B) Cadmium, (C) Silicon, (D) Sodium, (E) Manganese etc. Present in Mn Doped CdS Thin Film (Sample 3) with Magnification of 15,000. (Scale Bar: 2μm).

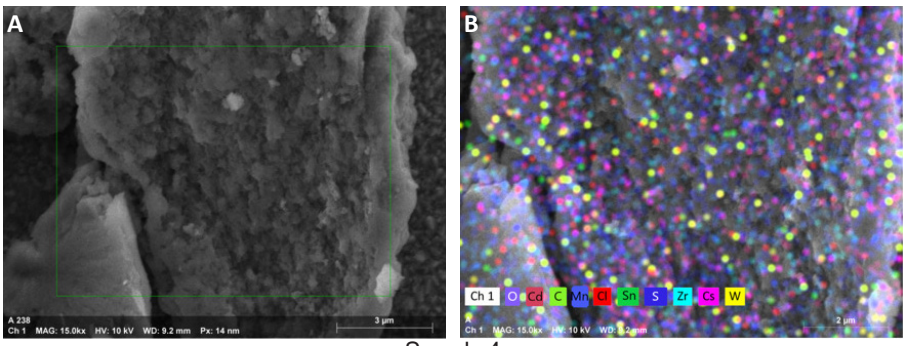

Figure 11. Mn Doped CdS Thin Film (Sample 4). (A) SEM Image with Magnification of 15,000, Scale Bar: 3μm, (B) SEM Image (Colour Image) with Magnification of 15,000. (Scale Bar: 2μm).

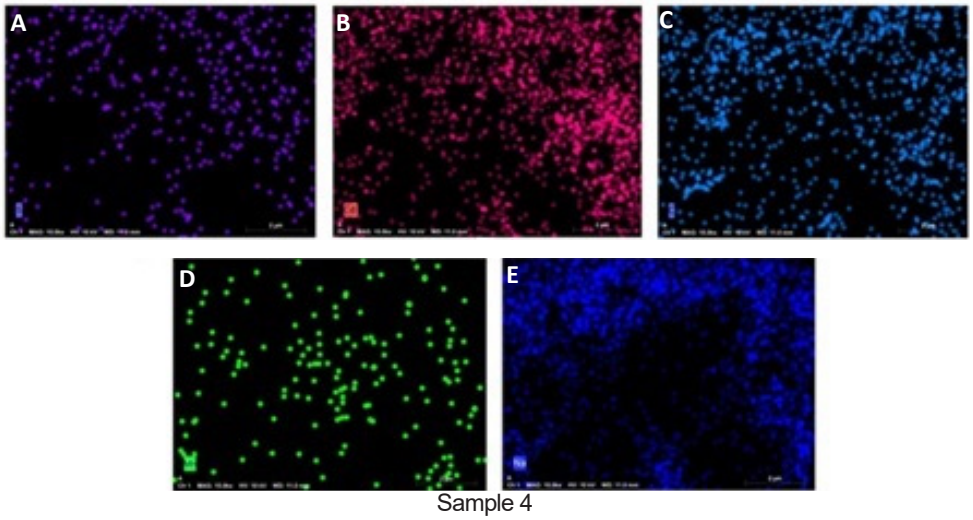

Figure 12. The Various Elements Present in Sample 4. (A) Sulphur, (B) Cadmium, (C) Carbon, (D) Manganese, (E) Sodium etc. Present in Mn Doped CdS Thin Film (Sample 4) with Magnification of 15,000. (Scale Bar: 2μm).

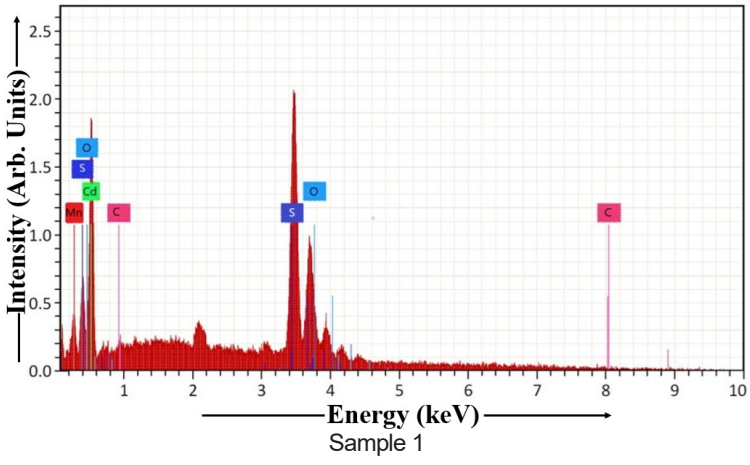

Figure 13. EDAX Spectrum of Mn Doped CdS Thin Film.

for CdS:Mn thin films (sample 3 and sample 4) are 4.72 and 4.96 respectively. From the values of Cd:S ratios of samples 1 and 2, it is clearly seen that the Cd:S ratio increases with increasing the dip time and decreasing the Mn concentration. The similar observation has been found in the case of samples 3 and 4[6,7]. The Cd:S ratio in CdS:Mn thin films increases with longer dip times and lower Mn concentrations during EDAX analysis because Mn ions are more likely to be incorporated at the film's surface, particularly under these conditions. This results in a shift in the detected composition towards more Cd-rich regions, effectively raising the Cd:S ratio in the analysis. Longer dip times allow more Cd and S ions to be deposited onto the substrate, potentially leading to a more uniform distribution of Cd and S throughout the film. However, at the surface, Mn ions may be preferentially incorporated

https://doi.org/10.53964/jmn.2025001

Table 1. EDAX of Mn Doped CdS Thin Film (Sample 1)

Element	At. No.	Netto.	Mass [%]	Mass Norm [%]	Atom [%]	abs. error [%] (1 sigma)	rel. error [%] (1 sigma
Manganese	25	625	1.27	1.29	5.77	0.36	27.96
Cadmium	48	6473	16.91	17.20	57.65	2.56	15.12
Sulphur	16	21390	61.95	63.00	28.46	2.14	3.45
Carbon	6	0	0.00	0.00	0.00	0.00	10.00
Oxygen	8	3111	11.22	11.41	4.80	0.47	4.23
Tin	50	2687	6.98	7.10	3.32	0.31	4.43
Sum			98.33	100.00	100.00		

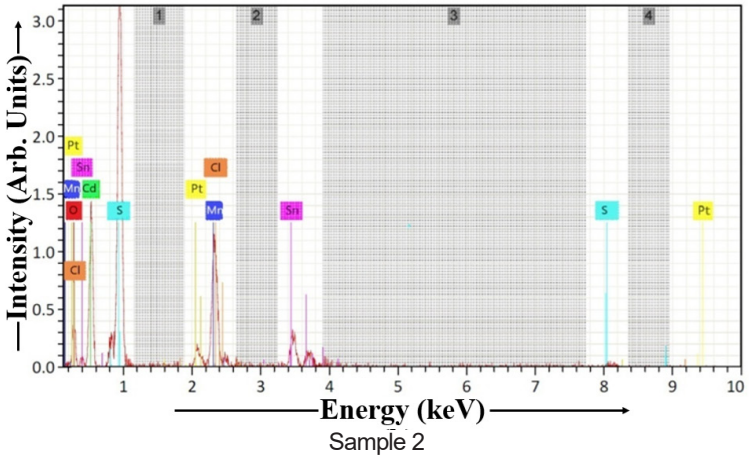

Figure 14. EDAX Spectrum of Mn Doped CdS Thin Film.

Table 2. EDAX of Mn Doped CdS Thin Film (Sample 2)

Element	At. No.	Netto.	Mass [%]	Mass Norm [%]	Atom [%]	abs. error [%] (1 sigma)	rel. error [%] (1 sigma
Oxygen	8	325	4.31	4.25	14.32	1.41	32.78
Cadmium	48	2173	15.05	14.83	47.56	2.82	18.75
Manganese	25	2160	7.58	7.47	1.99	0.37	4.83
Sulphur	16	7090	51.75	51.00	22.51	7.66	14.80
Tin	50	1352	12.43	12.25	5.18	0.61	4.88
Carbon	6	562	0.00	0.00	0.00	0.00	1.78
Chlorine	17	1423	10.34	10.19	8.44	0.53	5.12
Sum			101.46	100.00	100.00		

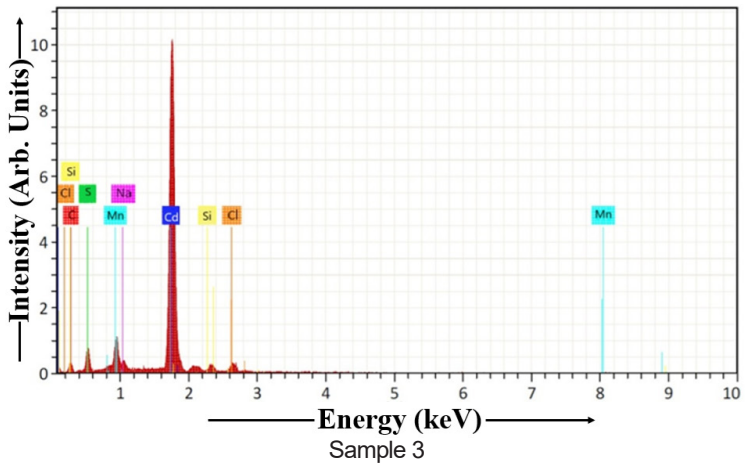

Figure 15. EDAX Spectrum of Mn Doped CdS Thin Film.

https://doi.org/10.53964/jmn.2025001

Table 3. EDAX of Mn Doped CdS Thin Film (Sample 3)

Element	At. No.	Netto.	Mass [%]	Mass Norm [%]	Atom [%]	abs. error [%] (1 sigma)	rel. error [%] (1 sigma
Carbon	6	0	0.00	0.00	0.00	0.00	10.00
Sulphur	16	1971	8.98	8.67	15.90	1.73	19.29
Cadmium	48	39425	74.45	71.87	75.13	3.10	4.16
Manganese	25	3200	11.82	11.41	5.27	2.04	17.28
Silicon	14	1209	5.32	5.13	0.74	0.30	5.58
Sodium	11	704	1.23	1.19	1.52	0.13	10.16
Chlorine	17	705	1.80	1.73	1.44	0.13	7.08
Sum			103.60	100.00	100.00		

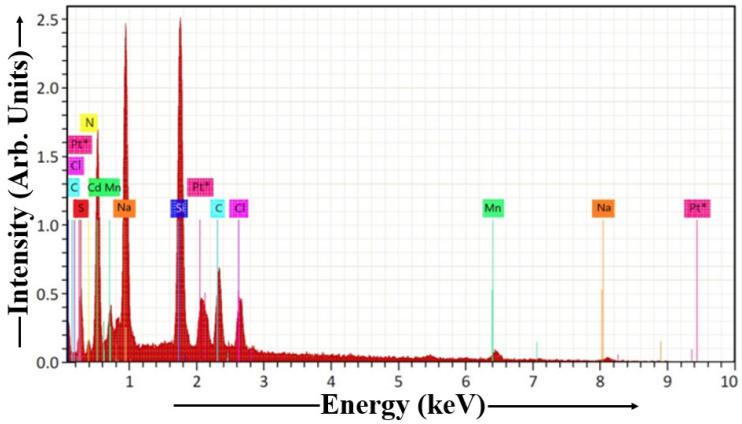

Sample 4

Figure 16. EDAX Spectrum of Mn Doped CdS Thin Film.

Table 4. EDAX of Mn Doped CdS Thin Film (Sample 4)

Element	At. No.	Netto.	Mass [%]	Mass Norm [%]	Atom [%]	abs. error [%] (1 sigma)	rel. error [%] (1 sigma
Sulphur	16	3984	9.36	11.77	14.34	1.55	16.60
Cadmium	48	14245	13.92	17.52	71.17	1.88	13.53
Silicon	14	30003	16.82	21.16	2.52	0.72	4.29
Carbon	6	7630	3.93	4.95	1.55	0.18	4.50
Chlorine	17	5254	3.12	3.93	2.68	0.15	4.65
Sodium	11	26132	25.83	32.49	2.28	3.25	12.57
Oxygen	8	935	2.01	2.53	4.85	0.49	24.32
Manganese	25	978	4.49	5.65	1.61	0.30	6.66
Sum			79.49	100.00	100.00		

due to their reactivity or preferred binding sites. Lowering the Mn concentration in the precursor solution means that less Mn is available for incorporation into the film. This leaves a higher proportion of Cd and S ions to be deposited, further increasing the likelihood of Cd-rich regions being analyzed. EDAX analysis) is sensitive to the elemental composition at the surface of the film. If Mn is preferentially localized at the surface, particularly when Mn is lower, the analysis will tend to report a higher Cd:S ratio, as the Cd:S ratio in the bulk might be different. The film's surface may have a slightly different composition than the bulk. Mn might be more concentrated at the surface, leading to a higher Cd:S ratio being reported by EDAX, which mainly analyzes the surface[6,7,18-22].

3.5 Ultraviolet-Visible Absorption Spectroscopy

With the help of UV-Vis spectrophotometer, the optical absorption spectra of CdS:Mn thin films (samples 1, 2, 3 and 4) were recorded ranging from 250 to 800nm. UV-Vis absorption spectra were obtained using a Shimadzu UV-300 double beam spectrometer at room temperature. The absorption spectra of Mn doped CdS thin films (samples 1 and 2) are shown in Figure 17.

https://doi.org/10.53964/jmn.2025001

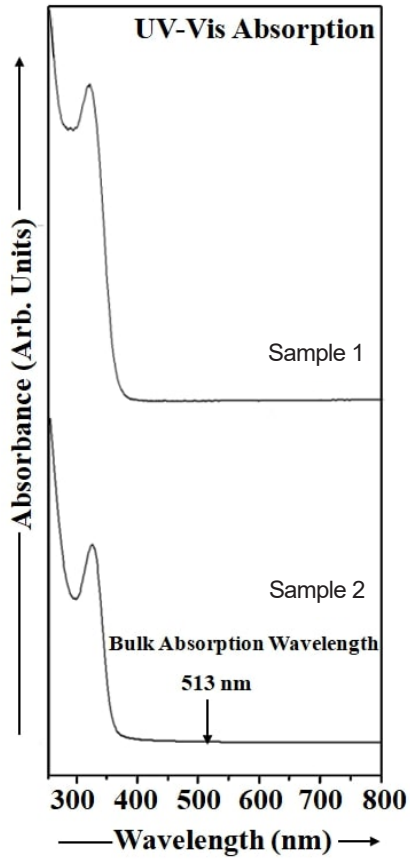

Figure 17. UV-Vis Absorption Spectra of Mn Doped CdS Thin Films (a) Sample 1 and (b) Sample 2.

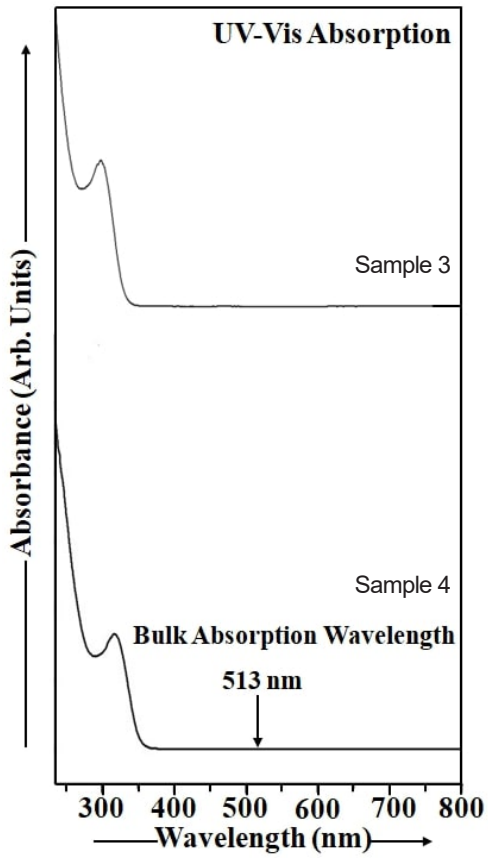

Figure 18. UV-Vis Absorption Spectra of Mn Doped CdS Thin Films (c) Sample 3 and (d) Sample 4.

The absorption peak had appeared at 300nm (energy gap ~ 4.14eV) in sample 1. The energy gap of the Mn doped CdS nanoparticles was estimated by using the Planck's quantum theory of radiation[23]. The particle size was calculated on the basis of effective mass approximation[24-26]. In sample 1, the particle size is 4.61nm. The amount of Mn incorporated in sample 1 is 0.154 At. Wt. %[6]. The absorption peak was observed at 325nm (energy gap ~ 3.82eV) in sample 2. The size of the CdS:Mn particles in sample 2 is 5.49nm. The atomic weight percentage of Mn element is 0.131%[6]. From the Figure 17, it can be clearly seen that the sharp excitonic peaks are visible in samples 1 and 2. The particle size depends on the concentration of the Mn element used in the synthesis of Mn doped CdS nanoparticles. There is a decrease in the particle size and an increase in the energy gap with increasing Mn concentration[6,7,27]. This indicates that there is a blue shift in the absorption wavelength with an increase in the Mn concentration[6,7,27] as compared to the bulk CdS material (513nm). Thus, the size quantization effect is observed in samples 1 and 2.

Figure 18 represents the absorption spectra of Mn doped CdS thin films (samples 3 and 4). The absorption peak was observed at 310nm (energy gap ~ 4.00eV) in sample 3. The particle size in sample 3 is 4.73nm. The atomic weight percentage of Mn element is 0.146 %[6].The optical absorption spectrum of sample 4 shows the absorption edge at 330nm (energy gap ~ 3.76eV). The size of the Mn doped CdS nanoparticles in sample 4 is 4.95nm. The amount of Mn incorporated in sample 4 is 0.137 At. Wt. %[6]. The sharpness of the absorption peaks of samples 3 and 4 is less than that of samples 1 and 2. The blue shift can be observed at smaller wavelengths in the absorption spectra of samples 3 and 4 with increasing Mn concentration as compared to the bulk material (513nm). Thus, the quantum size effect is observed in samples 3 and 4. From the above discussion, it is seen that the energy gap values of samples 1 and 2 are higher than those of samples 3 and 4. The optical band gap values obtained in our study (samples 1, 2, 3 and 4) are higher than those calculated in the previous literature[3,27,28]. The increased band gap due to smaller particle size (blue shift) and quantum confinement effect can be leveraged for applications requiring higher energy photons, such as in optoelectronics, solar cells, and photocatalysis. The blue shift means the absorption of higher energy photons. This shift is directly linked to the quantum size effect, where smaller nanoparticles have larger band gaps. Smaller CdS nanoparticles with increased band gaps can be used in LEDs and photodetectors to emit or detect light in the visible and near-infrared regions. The blue shift allows CdS nanoparticles to absorb a wider range of the solar spectrum, potentially improving the efficiency of solar cells. Increased band gap can lead to faster photocatalytic reactions, as more high-energy photons are absorbed. This can be beneficial in applications like water splitting or air purification.

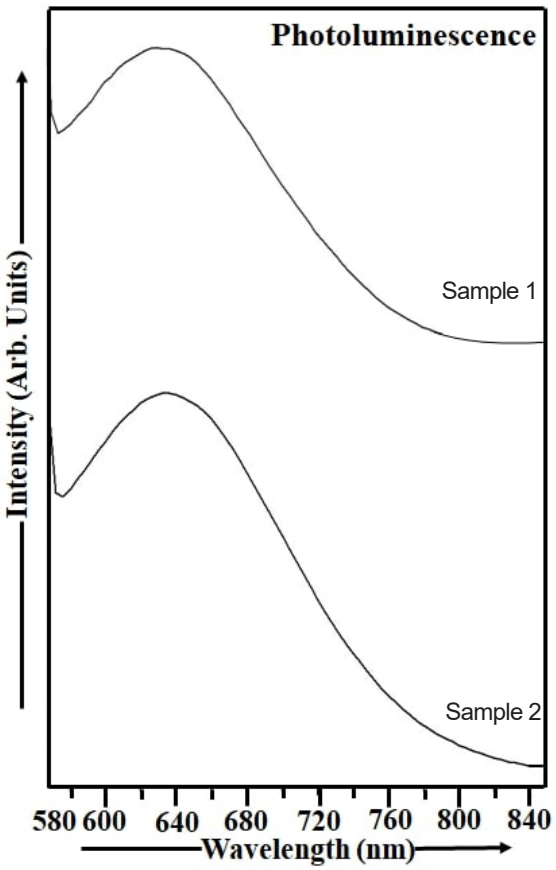

Figure 19. Photoluminescence Spectra of Mn Doped CdS Thin Films (a) Sample 1 and (b) Sample 2.

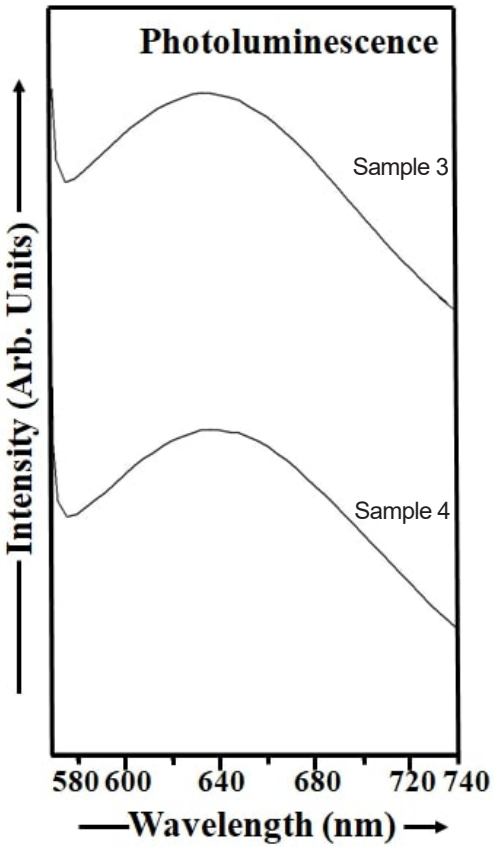

Figure 20. Photoluminescence Spectra of Mn Doped CdS Thin Films (c) Sample 3 and (d) Sample 4.

Doping with Mn can introduce new emission colors and efficiencies, further expanding the applications of CdS nanoparticles. Mn doping can also influence the electrical properties of CdS, leading to enhanced conductivity, which is beneficial for applications like electronic devices. By controlling the synthesis parameters, researchers can tailor the size of CdS nanoparticles to achieve specific optical and electronic properties. For example, smaller nanoparticles (with larger band gaps) can be used for applications requiring high-energy light absorption, while larger nanoparticles can be used for applications where longer wavelengths are desired. By connecting the observed trends in absorption spectra and quantum size effect to potential applications, the discussion can become more impactful and relevant, highlighting the practical significance of research on Mn-doped CdS nanoparticles[6,29-31].

3.6 Photoluminescence Spectroscopy

PL measurements were conducted using a Perkin Elmer LS – 50 fluorescence spectrometer, which utilized a xenon lamp for excitation. Figure 19 shows the PL spectra of Mn doped CdS thin films (samples 1 and 2) having 0.154 and 0.083 At. Wt. % Mn concentrations at room temperature. The appropriate filters were used to record the PL spectrum of sample 1 from 560 to 626nm in excitation mode and 626 to 850nm in emission mode. Also the PL spectrum of sample 2 was recorded from 567 to 633nm in excitation mode and 633 to 850nm in emission mode. The CdS:Mn particles (samples 1 and 2) were excited by using the excitation wavelengths of 570nm and 577nm respectively. The luminescence peak was observed at 628nm (energy gap ~ 1.98eV) in sample 1 and the luminescence peak was appeared at 636nm (energy gap ~ 1.95eV) in sample 2. The red shift was observed in the PL spectra of samples 1 and 2 in comparison with CdS bulk material (513nm). The intensity of the emission peak appearing at 628nm in sample 1 decreases with a decrease in particle size and an increase in Mn concentration[6,7].

The PL spectra of Mn doped CdS thin films (samples 3 and 4) having 0.154 and 0.083 At. Wt. % Mn concentrations at room temperature are shown in Figure 20. The excitation wavelength range used in sample 3 was 562 to 628nm and the emission wavelength range used in sample 3 was 628 to 850nm. Also the PL spectrum of sample 4 was recorded from 569 to 635nm in excitation mode and 635 to 850nm in emission mode. The CdS:Mn particles were excited at 572nm in sample 3 and at 579nm in sample 4. The emission peak had appeared at 630nm (energy gap ~ 1.97eV) in sample 3 and the emission peak was observed at 638nm (energy gap ~ 1.94eV) in sample 4. There is a red shift in the PL spectra of samples 3 and 4 as compared to the bulk material (513nm). Because of isolated Mn^{2+} ions, an orange emission had appeared at ~ 630nm in CdS:Mn nanoparticles (samples 1, 2, 3, 4). The photoluminescence (PL) efficiency can be enhanced by

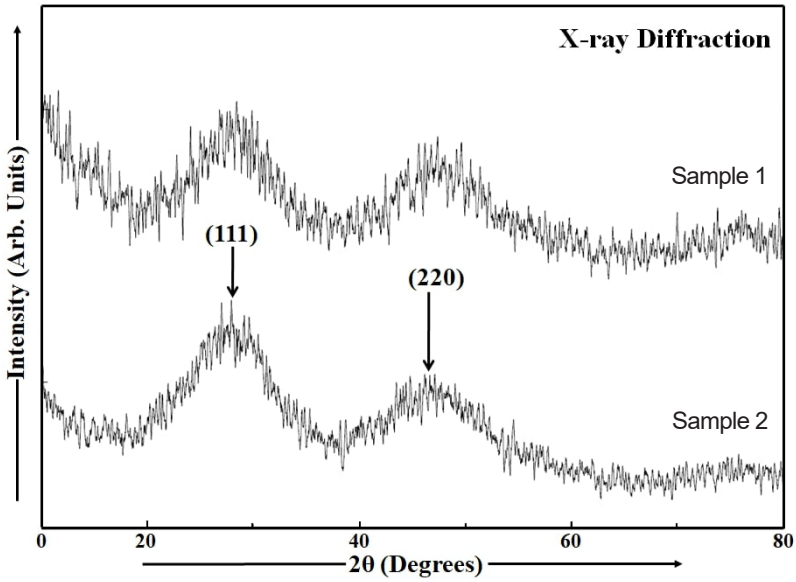

Figure 21. X-ray Diffraction Patterns of Mn Doped CdS Thin Films (a) Sample 1 and (b) Sample 2.

doping the CdS nanoparticles with Mn element and these Mn doped CdS nanoparticles can be used as fluorescent objects[6]. Mn doping alters CdS nanoparticles' band gap and emission characteristics, significantly impacting device performance, particularly in applications like solar cells and light-emitting devices. Mn doping can lead to changes in the band gap energy, affecting the material's ability to absorb light and generate charge carriers, and can also introduce new emission features, influencing the material's luminescent properties. Mn doping can decrease or increase the band gap energy of CdS. A decreased band gap can lead to better light absorption in the visible region, potentially improving the power conversion efficiency of solar cells. However, excessive doping can also reduce efficiency due to non-radiative recombination at Mn-related defects. Mn doping can introduce new emission features, like blue, green, and yellow emissions. These emissions can potentially improve the efficiency of multi-junction solar cells or be used for other applications. Mn doping can also alter the interface between CdS:Mn and other materials like P3HT:PCBM, affecting charge separation and transport. Mn doping can significantly enhance the luminescence of CdS, potentially leading to brighter and more efficient LEDs. The specific emission color can be tuned by controlling the Mn concentration and other parameters. Optimized Mn doping can improve the efficiency and stability of LEDs by reducing non-radiative recombination and enhancing the quality of the emission. Changes in the band gap and emission characteristics can affect the sensitivity and performance of photodetectors. Mn doping can introduce magnetic properties to CdS, which can be useful for spintronic devices. The concentration of Mn dopant significantly affects the band gap and emission properties. The method used for Mn doping can influence the morphology and properties of the CdS nanoparticles. Co-doping with other elements can further modulate the band gap and emission characteristics. The specific way in which the Mn-doped CdS nanoparticles are integrated into a device can impact its performance. In summary, Mn doping offers a powerful way to tailor the optical and electronic properties of CdS nanoparticles, making them suitable for a wide range of applications, including solar cells, LEDs, and other optoelectronic devices[6,7,32-40].

3.7 X-ray Diffraction

Powder X-ray diffraction analysis was carried out with a Philips PW 1840 diffractometer. The X-ray diffraction patterns of Mn doped CdS thin films (samples 1 and 2) are shown in Figure 21. The two broad XRD peaks are observed at 2θ values of 29.320° and 46.260° in sample 1 and at 2θ values of 27.820° and 46.860° in sample 2. Figure 22 represents the X-ray diffraction patterns of Mn doped CdS thin films (samples 3 and 4). The two broad XRD peaks are appeared at 2θ=28.460° and 2θ=48.560° in sample 3 and at 2θ=27.620° and 2θ=47.480° in sample 4. The XRD spectra of samples 1, 2, 3 and 4 range from 5° to 80°. The two broad peaks indicating.

The formation of nano sized particles are observed in samples 1, 2, 3 and 4. These peaks refer to the planes (111) and (220) which indicate the zinc blende structure[3,6,27]. The average size (d') of CdS:Mn nanoparticles was estimated by using the Debye-Scherrer formula, $d' = \frac{0.9\lambda}{\beta cos\theta}$[41]. The average particle sizes of samples 1, 2, 3 and 4 are 4.11nm, 4.09nm, 4.10nm and 4.09nm respectively. The values of strain (ε) and dislocation density (δ) of CdS:Mn nanoparticles were calculated by using the formulae ε=βcosθ/4 and δ=1/d'^{2}respectively[42]. The values of ε of CdS:Mn nanoparticles (samples 1, 2, 3 and 4) are 8.440×10^{-3}m, 8.469×10^{-3}m, 8.457×10^{-3}m and 8.472×10^{-3}m respectively and the values of δ of CdS:Mn nanoparticles (samples 1, 2, 3 and 4) are 5.92 x 10^{16} lines/m^2, 5.98×10^{16} lines/m^2, 5.95×10^{16} lines/

https://doi.org/10.53964/jmn.2025001

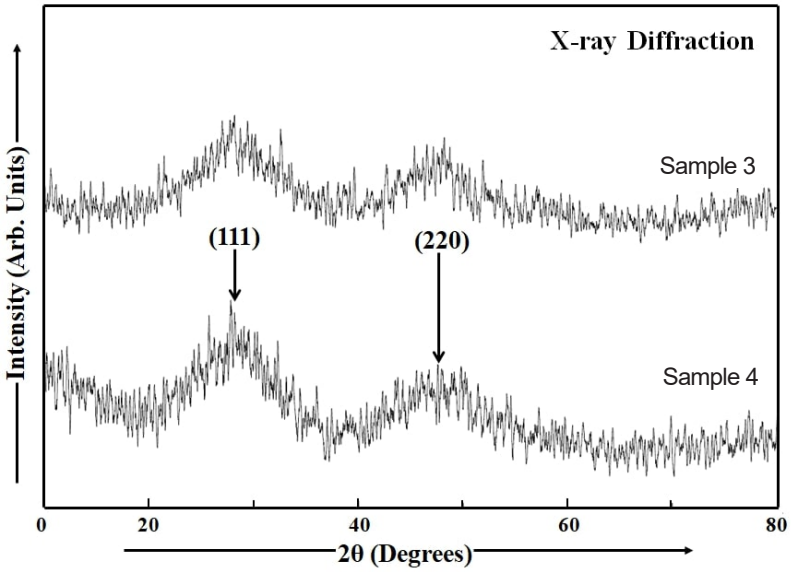

Figure 22. X-ray Diffraction Patterns of Mn Doped CdS Thin Films (c) Sample 3 and (d) Sample 4

m^2 and 5.98×10^{16} lines/m^2respectively. The incorporation of Mn element in the host CdS lattice does not change the phase which is shown by the XRD spectra of samples 1, 2, 3 and 4. The phases related to impurities were not detected[3]. According to Vegard's law, an individual XRD peak cannot be generated by the dopant near the host peak but the shift in the position of the host peak can be produced by the dopant,[3]. The lattice parameter (α) of cubic unit cell was calculated by using the Bragg's law (n λ=2 d sin θ) for the CdS:Mn nanoparticles,

$$\frac{1}{d_{hkl}^2}=\frac{h^2+k^2+l^2}{\alpha^2}(1)$$

$$\alpha=\frac{\lambda}{2sin\theta}\sqrt{h^2+k^2+l^2}(2)$$

The replacement of larger Cd^{2+} ions by the incorporation of smaller Mn^{2+} ions in cubic host CdS lattice structure explained that the volume of the unit cell lattice decreases with an increase in Mn concentration[3]. The XRD patterns of Mn doped CdS nanoparticles are perfectly equivalent to those reported in JCPDS (Joint Committee on Powder Diffraction Standards) data for cubic CdS[43].

The choice of substrate material significantly impacts the crystalline quality and orientation of thin films, including CdS:Mn films with a cubic zinc blend structure. Substrate properties like lattice mismatch, surface morphology, and thermal properties can induce strain and affect film growth, ultimately influencing crystallinity and preferred orientation. A large lattice mismatch between the substrate and the growing CdS:Mn film can induce significant strain, leading to lattice distortions and defects within the film. This can result in a reduction in crystalline quality, as the film may not be able to perfectly accommodate the lattice mismatch, leading to a polycrystalline or even amorphous structure. In contrast, a smaller lattice mismatch can promote epitaxial growth, where the film's crystal structure is aligned with the substrate, resulting in a highly crystalline and oriented film. Substrate surface roughness can influence the nucleation density and growth direction of the film. A rough surface can provide more nucleation sites, leading to a more polycrystalline film with a random orientation. A smooth surface, on the other hand, can promote the growth of larger, more aligned crystals, leading to a highly crystalline and oriented film. Surface topography, such as steps or terraces, can also affect the film's orientation, as the film's growth may be influenced by the substrate's surface features. The thermal expansion coefficient of the substrate can affect the film's internal stress as the temperature changes during and after deposition. A large difference in thermal expansion coefficients between the substrate and the film can introduce significant thermal stress, which can lead to cracking, deformation, or delamination of the film. To minimize thermal stress, it's important to choose a substrate with a thermal expansion coefficient that is relatively close to that of the CdS:Mn film. Glass substrates are commonly used due to their low cost and ease of preparation. However, they often have a non-ideal surface, which can lead to a less crystalline and more polycrystalline CdS:Mn film. Silicon substrates have a relatively high thermal expansion coefficient and a good lattice match with many II-VI semiconductors, making them suitable for growing high-quality films. The choice of other substrates depends on specific applications and the desired film properties. For example, GaAs substrates are suitable for electronic applications, while MgO substrates are used for optical applications.In summary, substrate selection plays a critical role in determining the crystalline quality and orientation of CdS:Mn thin films. By carefully considering the substrate's lattice mismatch, surface morphology, thermal properties, and other factors, researchers can optimize film growth and achieve desired film properties[6,44-53].

Substrate type can significantly influence the crystalline quality and orientation of CdS:Mn thin films deposited on FTO glass substrates and silicon wafers. FTO glass,

with its inherent structure, can promote certain preferred orientations in the CdS:Mn film, leading to enhanced crystalline quality and potentially different optoelectronic properties. Silicon wafers, being single-crystalline, can also induce preferential growth, but may not always result in the same orientation as FTO glass.FTO glass, a transparent conducting oxide, has a glass matrix with a specific structure that can guide the growth of the CdS:Mn film. The FTO layer itself can act as a template, encouraging the deposition of CdS:Mn in a particular orientation. This can result in a sharper, more intense XRD peak, indicating a better degree of crystalline alignment and potentially higher crystallite size. Silicon wafers, being single-crystal materials with a well-defined lattice structure, can also influence the orientation and crystallinity of the deposited CdS:Mn film. The lattice mismatch between the CdS:Mn film and the silicon substrate can lead to the formation of defects and strain. However, the silicon substrate can still encourage the growth of oriented films, potentially leading to different preferred orientations compared to FTO glass. The type of substrate can affect the crystalline quality of the CdS:Mn thin film by influencing factors like grain size, orientation, and the presence of defects. For example, FTO glass substrates might promote the growth of larger, more aligned grains compared to silicon substrates, resulting in a higher quality film. The preferred orientation of the CdS:Mn film is also influenced by the substrate. FTO glass might encourage growth along specific crystallographic planes (e.g., (100) plane) while silicon substrates might lead to different preferred orientations. Studies have shown that CdS thin films deposited on FTO substrates exhibit a sharper XRD peak with a higher intensity compared to films deposited on silicon wafers. This indicates a better crystallinity and a preferred orientation on the FTO substrate. Conversely, films on silicon wafers may show a weaker, broader peak, suggesting a lower degree of crystallinity and possibly different orientations[6,50,54-58].

Mn doped CdS nanoparticles and their thin films, especially when prepared via dip coating, are used in diverse applications due to their enhanced optical and structural properties. These improvements, observed in UV-Vis absorption, PL, and morphological/structural characterizations (XRD, SEM, EDAX, TEM, AFM), make them suitable for solar cells, sensors, and other optoelectronic devices. Mn doping can alter the optical band gap of CdS, affecting its light absorption characteristics. This can be crucial for applications like solar cells, where the ability to absorb specific wavelengths of light is important. Mn ions in CdS can introduce new emission wavelengths, potentially enhancing the material's luminescence capabilities. This is important for applications like light-emitting devices. XRD, SEM, EDAX, TEM, AFM techniques provide insights into the morphology, composition, and structure of the nanoparticles and thin films. These characterizations help understand the effects of Mn doping on the material's properties and how they are preserved during the dip coating process. Provides surface morphology information, while EDAX helps determine the elemental composition.TEM and AFM offer more detailed information about the microstructure and surface topography of the materials. XRD Helps identify crystalline phases and determine the crystal structure. Mn doping can improve the stability and resistance to photodegradation of CdS nanoparticles. Mn ions can enhance electron conduction, potentially leading to improved current density (Jsc) in solar cells. The enhanced optical properties and improved charge transport make Mn doped CdS materials promising for use in solar cells, according to a study on Mn doped CdS quantum dots as sensitizers. The material's ability to absorb and interact with gases can be utilized in gas sensing applications. The modified optical properties can be used to design efficient photodiodes and light-emitting diodes, according to a study on nanocrystalline CdS thin films. Dip coating is a simple and cost-effective method for depositing thin films. This method allows for reproducible and controlled film deposition. It enables the formation of thin films with uniform thickness and good adhesion to the substrate. In essence, the combination of Mn doping for enhanced properties and the controlled thin-film deposition via dip coating makes these materials versatile for various applications, especially in the field of optoelectronics[6,9,59-63].

4 CONCLUSION

Mn doped CdS nanoparticles with varying manganese concentration were synthesized by wet chemical reaction route using thioglycerol as the capping agent. CdS:Mn thin films were prepared by the deposition of Mn doped CdS nanoparticles on FTO glass substrates (sample 1 and sample 2) and also on silicon wafers (sample 3 and sample 4) by the dip coating technique. These thin films were analysed by AFM, TEM, SEM, EDAX and Mapping. Highly dense rectangular clusters are present in CdS:Mn thin films. The presence of the clusters and the increment in the cluster size with increasing dip time are shown in the AFM images of those films. The ring patterns shown by the SAED images of CdS:Mn thin films indicate the polycrystalline nature of those films. An increment in the sizes of the spherical clusters is observed in the TEM images of thin films at different magnifications. Increments in the grain size with increasing dip time and a decrease in the crystal defects caused by the heat treatment in air atmosphere are shown by the SEM images of Mn doped CdS thin films. The EDAX analysis shows the stoichiometric nature of thin films. The blue shift is observed in the UV-Vis absorption spectra and the red shift is observed in the PL spectra of CdS:Mn thin films (samples 1, 2, 3 and 4). The cubic crystal structure of Mn doped CdS nanoparticles (samples 1, 2, 3 and 4) is shown by the XRD investigation. A similarity is observed between the characterization results of thin films prepared by the deposition of CdS:Mn nanoparticles on

FTO glass substrates and on silicon wafers. Mn doped CdS thin films can be used in the fabrication of photovoltaic and optoelectronic devices due to their semiconducting nature.

Acknowledgements

The authors are extremely grateful to the Head of the Physics Department and the Head of the Chemistry Department of Savitribai Phule Pune University and also the operators from IIT Powai, Mumbai for providing the necessary help in carrying out the characterizations.

Conflicts of Interest

The authors declare that there is no conflict of interest.

Data Availability

All data generated or analyzed during this study are included in this published article and its supplementary information files.

Author Contribution

Darekar MS was the main author, designed the experiments, conducted the practical work, interpretation of results, drawing diagrams and tables, and wrote the paper. Praveen BM supervised the manuscript preparation process.

Abbreviation List

AFM, Atomic Force Microscopy
A.R., Analytical Reagent
CdS, Cadmium Sulphide
CdS:Mn, Mn doped CdS
DMS, Diluted Magnetic Semiconductor
EDAX, Energy Dispersive Analysis by X-rays
FTO, Fluorine doped Tin Oxide
Mn, Manganese
PL, Photoluminescence
SAED, Selected Area Electron Diffraction
SEM, Scanning Electron Microscopy
TEM, Transmission Electron Microscopy
UV-Vis, Ultraviolet-Visible
XRD, X-ray diffraction

References

[1] Venkatesu P. International Conference on Advanced Nanomaterials & Emerging Engineering Technologies (ICANMEET), Chennai, India, 24-26 July 2013.

[2] Gadalla AA, Aboelkhir AN, Mahesha MG et al. Synthesis and characterization of Mn-Doped CdS-diluted magnetic semiconductor nanoparticles. *J Mater Sci Mater Electron,* 2020; 31: 10941.[DOI]

[3] Gadalla A, Almokhtar M, Abouelkhir AN. Effect of Mn doping on structural, optical and magnetic properties of CdS dilute magnetic semiconductor nanoparticles. *Chalcogenide Lett*, 2018; 15: 207-218.

[4] Maity P, Kumar R, Jha SN et al. Investigation of the Physical Properties of Mn-doped CdS Diluted Magnetic Semiconductor Quantum Dots: Non-linear Band Gap Variation With Downwards Bowing. Available at SSRN 4066164, 2022.[DOI]

[5] Venkatesu P, Ravichandran K. Manganese doped cadmium sulphide (CdS:Mn) quantum particles: Topological, photoluminescence and magnetic studies. *Adv Mater Lett,* 2013; 4: 202-206.[DOI]

[6] Darekar MS, Praveen BM. Hyperfine Splitting and Ferromagnetism in CdS:Mn Nanoparticles for Optoelectronic Device Applications. *J Semicond*, 2023; 44: 122502.[DOI]

[7] Darekar MS, Praveen BM. Preparation of manganese doped copper sulphide nanoparticles by cost-favourable chemical method at room temperature. *J metastable nanocrystalline Mater*, 2025; 41: 43-57.[DOI]

[8] Darekar MS, Praveen BM. Synthesis and characterization of nanopoarticles of semiconducting metal sulphide and their application. *Phys Scr*, 2022; 97: 065805.[DOI]

[9] Darekar MS, Praveen BM. Effects of Heat Treatment in Air Atmosphere on Dip Coating Deposited CdS Thin Films for Photo Sensor Applications. *J Mod Nanotechnol*, 2023; 3: 2.[DOI]

[10] Darekar MS, Praveen BM. High Photosensitivity Nanocrystalline p-Cu_2S/n-FTO Heterojunction Photodetectors Prepared by Dip Coating Method. *J Mod Nanotechnol*, 2023; 3: 1.[DOI]

[11] Bisen DP, Brahme N, Sharma R et al. Effect Of Temperature On The Synthesis Of CdS:Mn Doped Nanoparticles. *Chalcogenide Lett*, 2009; 6: 427.

[12] Tiwary CS, Sarkar R, Kumbhakar P et al. Synthesis and optical characterization of monodispersed Mn^{2+} doped CdS nanoparticles. *Phys Lett A*, 2008; 372: 5825.[DOI]

[13] Marandi M, Taghavinia N, Sedaghat Z et al. Thermochemical growth of Mn-doped CdS nanoparticles and study of luminescence evolution. *Nanotechnol*, 2008; 19: 225705.[DOI]

[14] Marandi M, Taghavinia N, Iraji A et al. Self-assembled one-pot synthesis of red luminescent CdS:Mn/$Mn(OH)_2$ nanoparticles. *J Lumin*, 2008; 128: 1980.[DOI]

[15] Salimian S, Shayesteh SF. Luminescence Properties of Manganese Doped CdS Nanoparticles under Various Synthesis Conditions. *Acta Phys Pol A*, 2010; 118: 633.[DOI]

[16] Vidhya Raj DJ, Linet JM, Das SJ. Synthesis and Characterization of 1-thioglycerol capped CdSe and Cu (copper) doped CdSe nanoparticles at Room Temperature. *Int J Chemtech Res*, 2014; 6: 2042.

[17] Khimani AJ, Chaki SH, Malek TJ et al. Cadmium sulphide (CdS) thin films deposited by chemical bath deposition (CBD) and dip coating techniques—a comparative study. *Mater Res Express*, 2018; 5: 036406.[DOI]

[18] Phasook N, Kamoldirok S, Yindeesuk W. Optical properties of Mn-doped CdS thin films grown by the SILAR method. *J*

Phys Conf Ser, 2018; 1144: 012009.[DOI]

[19] Ghosh PK, Saha B, Chattopadhyay KK. Effect of deposition time on optical properties of nanocrystalline CdS thin films synthesized via rf- Sputtering technique**.** Source IEEE Xplore: Conference: Physics of Semiconductor Devices, 2007. IWPSD 2007. International Workshop on, January 2008.[DOI]

[20] Bakly AAK, Spencer BF, O'Brien P. The deposition of thin films of cadmium zinc sulfide $Cd_{1-x}Zn_xS$ at 250 °C from spin-coated xanthato complexes: a potential route to window layers for photovoltaic cells. *J Mater Sci*, 2018; 53: 4360.[DOI]

[21] Ochang MB, Ahemen I, Amah AN et al. Effect of substrate temperature on the structural optical and electrical properties of new $Cu_2Cd_{0.8}Mn_{0.2}SnS_4$ photo-absorber layer for solar cells. *Results Opt*, 2023; 13: 100509.[DOI]

[22] Radovanovic PV, Barrelet CJ, Gradecak S et al. General Synthesis of Manganese-Doped II−VI and III−V Semiconductor Nanowires. *Nano Lett*, 2005; 5: 1407.[DOI]

[23] Suresh SR. Studies on the dielectric properties of CdS nanoparticles. *Appl Nanosci,* 2013; 4: 325-329.[DOI]

[24] Brus LE. A simple model for the ionization potential, electron affinity, and aqueous redox potentials of small semiconductor crystallites. *J Chem Phys*, 1983; 79: 5566-5571.[DOI]

[25] Brus LE. Electron–electron and electron-hole interactions in small semiconductor crystallites: The size dependence of the lowest excited electronic state. *J Chem Phys*, 1984; 80: 4403-4409.[DOI]

[26] Brus L. Electronic wave functions in semiconductor clusters: Experiment and theory. *J Phys Chem*, 1986; 90: 2555-2560.[DOI]

[27] Patle US, Ahirwar RK, Bhatt A et al. Enhanced Photoluminescence Properties of Mn doped CdS nanocrystals. *AIP Conf Proc*, 2019; 2100: 020165.[DOI]

[28] Stojic BB, Milivojevic D, Comor M et al. Optical and electron paramagnetic resonance spectroscopy of $Cd_{1-x}Mn_xS$ quantum dots. *J Phys:Condens Matter*, 2004; 16: 4625-4633.[DOI]

[29] Kaur M, Sharma A, Erdem O et al. Understanding the suitable alloying conditions for highly efficient Cu- and Mn-doped $Zn_{1-x}Cd_xS$/ZnS core-shell quantum dots. *Opt Mater*, 2023; 145: 114471.[DOI]

[30] Vatankhah C, Saki M, Jafargholinejad S. Theoretical and Experimental Investigation of Quantum Confinement Effect on the Blue Shift in Semiconductor Quantum Dots. *Orient J Chem,* 2015; 31: 907-912.[DOI]

[31] Torimoto T, Kameyama T, Uematsu T et al. Controlling optical properties and electronic energy structure of I-III-VI semiconductor quantum dots for improving their photofunctions. *J Photoch Photobio C*, 2023; 54: 100569.[DOI]

[32] W-Rodriguez FJ, C-Urbiola IR, H-Landaverde MA et al. Effects of incorporating manganese in CdS thin films elaborated by CBD and the performance of Schottky diodes TCO/CdS:Mn/C. *Mater Chem Phys*, 2024; 312: 128636.[DOI]

[33] Devadoss I, Muthukumaran S. Band gap tailoring and yellow band emission of $Cd_{0.9-x}Mn_xZn_{0.1}S$ (x=0 to 0.05) nanoparticles: Influence of Mn concentration. *Mater Sci Semicond Process*, 2016; 41: 282.[DOI]

[34] B-Chory C, Dem C, Remenyi C et al. Synthesis and characterization of manganese-doped CdS nanoparticles. *Phys Chem Chem Phys*, 2003; 5: 1639.[DOI]

[35] Azab AA, Ibrahim RS, Seoudi R. Investigating the effects of Mn content on the morphology and dielectric properties of CdS nanoparticles. *Appl Phys A*, 2024; 130: 294.[DOI]

[36] Devi LS, Devi KN, Sharma BI et al. Influence of Mn doping on structural and optical properties of CdS nanoparticles. *Ind J Phys*, 2014; 88: 477-482.[DOI]

[37] Nag A, Sarma DD. White Light from Mn^{2+}-Doped CdS Nanocrystals: A New Approach. *J Phys Chem*, 2007; 111: 13641.[DOI]

[38] Bera D, Qian L, Tseng TK et al. Quantum Dots and Their Multimodal Applications: A Review. *Mater*, 2010; 3: 2260.[DOI]

[39] Mehmood I, Liu Y, Chen K et al. Mn doped CdS passivated $CuInSe_2$ quantum dot sensitized solar cells with remarkably enhanced photovoltaic efficiency. *RSC Adv*, 2017; 7: 33106.[DOI]

[40] Darvishi M, Nikfarjam A. A Novel Thermochemical Method for Fabrication and Theoretical Explanation of High Luminescent Mn-Doped CdS Nanoparticles. *J Mater Sci Chem Eng*, 2018; 6: 1-20.[DOI]

[41] Al-Taay HF. Preparation and Characterization of Chemical Bath Deposition Synthesis CdS Nanocrystalline Thin Films. *Iraqi J Sci*, 2017; 58: 454-461.[DOI]

[42] Chowdhury RI, Hossen MA, Mustafa G et al. Characterization of chemically deposited cadmium sulfide thin films. *Int J Mod Phys B*, 2010; 10: 5901-5911.[DOI]

[43] Saraf R. High Efficiency and cost effective Cu_2S/CdS thin-film solar cell. *IOSR-JEEE*, 2012; 2: 47-51.[DOI]

[44] Emir C, Tataroglu A, Gokmen U et al. Analysis of the structural and optical characteristics of ZnSe thin films as interface layer. *J Mater Sci Mater Electron*, 2025; 36: 1-12.[DOI]

[45] Acosta-Silva YJ, Méndez-López A, de Moure-Flores F et al. Characterization of substitutional and interstitial Eu^{+3}-positions in CdS lattice. *Mater Chem Phys*, 2021; 257: 123763.[DOI]

[46] Ma L, Ai X, Wu X. Effect of substrate and Zn doping on the structural, optical and electrical properties of CdS thin films prepared by CBD method. *J Alloy Compd*, 2017; 691: 399-406.[DOI]

[47] Joishy S, Poornesh P, Choudhary RJ et al. Influence of Cd on Structure, Surface Morphology, Optical and Electrical Properties of Nano Crystalline ZnS Films. *SENSOR ACTUAT A-PHYS*, 2019; 303: 111719.[DOI]

[48] Morelos-Medina LF, Nava-Mendoza R, Cortés-Romero CM et al. Influence of Zn in the CdS Crystal Lattice and Its Impact over the Catalytic Activity in the H_2 Production. *J Chem*, 2022; 2022: 5567247.[DOI]

[49] Khan AUR, Ramzan M, Iqbal MF et al. Effect of the Source-to-Substrate Distance on Structural, Optoelectronic, and Thermoelectric Properties of Zinc Sulfide Thin Films. *Materials*, 2022; *15:* 8047.[DOI]

[50] Arsad AZ, Zuhdi AWM, Abdullah SF et al. Effect of Chemical Bath Deposition Variables on the Properties of Zinc Sulfide Thin Films: A Review. *Molecules*, 2023; 28: 2780.[DOI]

[51] Popa ME. Morphological, structural, compositional and raman characterization of ZnSXSe1-X thin films deposited by quasi-closed volume technique. *Chalcogenide Lett*, 2018; 15: 441.

[52] Raha S, Ahmaruzzaman Md. ZnO nanostructured materials and their potential applications: progress, challenges and

perspectives. *Nanoscale Adv*, 2022; 4: 1868.[DOI]

[53] Wojciechowski P, Lewandowski M. Iron Nitride Thin Films: Growth, Structure, and Properties. *Cryst Growth Des*, 2022; 22: 4618.[DOI]

[54] Moualkia H, Hariech S, Aida MS et al. Growth and physical properties of CdS thin films prepared by chemical bath deposition. *J Phys D: Appl Phys*, 2009; 42: 135404.[DOI]

[55] Pathan HM, Lokhande CD. Deposition of metal chalcogenide thin films by successive ionic layer adsorption and reaction (SILAR) method. *Bull Mater Sci*, 2004; 27: 85.[DOI]

[56] Rekha SM, Neelamana HV, Bhat SV. Recent Advances in Solution-Processed Zinc Oxide Thin Films for Ultraviolet Photodetectors. *ACS Appl Electron Mater*, 2023; 5: 4051.[DOI]

[57] Dey A, Ye J, De A et al. State of the Art and Prospects for Halide Perovskite Nanocrystals. *ACS Nano*, 2021; 15: 10775.[DOI]

[58] Alshammari BH, Lashin MMA, Mahmood MA et al. Organic and inorganic nanomaterials: fabrication, properties and applications. *RSC Adv*, 2023; 13: 13735.[DOI]

[59] Sharma B, Lalwani R, Das R. Nanocrystalline CdS thin films deposited by sol-gel spin coating method: Effect of aging and doping on structural, optical, and electrical properties. *Optik*, 2023; 281: 170831.[DOI]

[60] Carrasco-Chavez LA, Rubio-Valle JF, Jiménez-Pérez A et al.. Study of CdS/CdS Nanoparticles Thin Films Deposited by Soft Chemistry for Optoelectronic Applications. *Micromachines*, 2023; 14: 1168.[DOI]

[61] Darekar MS, Praveen BM. Chemical synthesis of Lead Iodide nanoparticles for photovoltaic and optoelectronic device applications. *Int J Nano Dimens*, 2024; 15: 1.

[62] Alghoraibi I. Influence of the DEA Concentration on Structural and Optical Properties of Nanodot PbS Thin Films Growth by Chemical Solution Deposition: Unveiling Dual Optical Absorption Edges. *J Nanomater*, 2024; 2024: 9504522.[DOI]

[63] Shakil MA, Das S, Rahman MA et al. A Review on Zinc Sulphide Thin Film Fabrication for Various Applications Based on Doping Elements. *Mater Sci Appl*, 2018; 9: 751-778.[DOI]